Journal of Zhejiang University-SCIENCE A (Applied Physics & Engineering)
ISSN 1673-565X (Print); ISSN 1862-1775 (Online)
www.zju.edu.cn/jzus; www.springerlink.com
E-mail: jzus@zju.edu.cn

Mechanical and magnetic hysteresis as indicators of the origin and inception of fatigue damage in steel*

Sheng BAO, Wei-liang JIN, Ming-feng HUANG†‡

(*Institute of Structural Engineering, Zhejiang University, Hangzhou 310058, China*)

†E-mail: mfhuang@zju.edu.cn

Received Apr. 16, 2010; Revision accepted June 22, 2010; Crosschecked July 16, 2010

Abstract: N_2 and N_3 are known as the transition points of the three principal stages of fatigue: initial accommodation, accretion of damage and terminal fatigue. Many experiments show that the ratios of N_2/N_f and N_3/N_f tend to be stable even though the specific N_2 and N_3 values may fluctuate widely. The primary goal of this research is to study the piezomagnetic field surrounding AISI 1018 steel specimen under repeated loads and to find the ratio values of N_2/N_f and N_3/N_f by analyzing 11 sets of low-cycle fatigue data. An MTS-810 testing system with a peak capacity of 222 kN was used to obtain the data which consisted of stress, strain, and piezomagnetic field. A computer program was constructed to track the evolution of the piezomagnetic field and regression analysis was carried out to determine N_2 and N_3 values. It was observed that there exists a consistent relationship between N_2 and N_f. The apparent invariance of the ratio N_2/N_f implies that N_2 may be identified as an index of performance in the early loading response of a specimen that forecasts its fatigue life, N_f. It has been demonstrated that measurements of the magnetic and mechanical hysteresis can yield significant insights into the various stages of the development of a fatigue critical microstructure which culminates in complete rupture of the material.

Key words: Piezomagnetic effects, Fatigue damage, Mechanical hysteresis, Magnetic hysteresis
doi:10.1631/jzus.A1000178 **Document code:** A **CLC number:** TB302.5

1 Introduction

Metal fatigue is a result of a cumulative damage process due to repeated cyclic loadings which can cause premature and unpredictable failure (Kachanov, 1986; Lemaitre and Chaboche, 1990; Bily, 1993; Erber, 2001). It is a complicated metallurgical process at the microscopic level which is difficult to explain accurately or model (Bannantine *et al.*, 1990). Despite the complexities, great efforts have been put into industrial environments and in research laboratories to detect the destructive degradation process of fatigue in metals.

Piezomagnetism refers to a change in the magnetization of a material when it is subjected to mechanical stress. It was first investigated by Villari (1865). He discovered that when an iron bar is weakly magnetised and subjected to longitudinal tension, the magnetic induction increases. However, when the iron bar is strongly magnetised, the effect of tension will decrease the magnetic induction (Becker and Doring, 1939; Bozorth, 1951). In the case of cobalt, the effect is opposite to that in iron, that is, when the cobalt bar is weakly magnetised, the effect of pull will decrease the magnetic induction. The Villari effect is the reciprocal effect of magnetostriction which concerns with the changes in dimension of a ferromagnetic material when subjected to a magnetising field (Cullity, 1972).

2 Experiment

An MTS-810 servo-hydraulic testing machine with a peak capacity of 222 kN was used to apply

‡ Corresponding author

* Project supported by the National Natural Science Foundation of China (No. 50901067), and the Technological Research and Development Programs of the Ministry of Railways (No. 2010G007-E), China

© Zhejiang University and Springer-Verlag Berlin Heidelberg 2010

push-pull loading. The principal components of this testing machine include MTS 458.20 MicroConsole, hydraulic power supply, load unit and servo controller. A high performance computer was used to undertake data acquisition and analysis. This testing system is able to produce triangular, rectangular or sine waves with programs entered into its microprofiler. In this research, only triangular waveforms were used. Signals from the microprofiler are sent to the servovalve. After comparing the control signal from the MicroConsole (actual actuator position) with the command signal (desired actuator position) in terms of voltage, the servovalve moves the actuator in the corresponding direction to eliminate the voltage difference. This servovalve movement gives accurate and reliable results for fatigue testing.

Before the experiment was started, great care was taken to ensure the correct installations of the specimen, the extensometer and the magnetometer probe. The specimen was first mounted on the lower grip, then using the MicroConsole, the actuator rod was extended to secure the specimen in the upper grip. With the upper grip locked, a standard 1.27-cm gauge length MTS extensometer was mounted directly on the specimen to measure strains. Over a maximum strain rage of ±0.15, the hysteresis and nonlinearity of the gauge are 0.10% and 0.15%, respectively. To eliminate magnetic interference, rubber bands instead of steel springs were used to install the extensometer. In this research, magnetic signals were detected by an APS 428D fluxgate magnetometer probe. It was fixed in the lower grip of the load unit by a non-magnetic support (Fig. 1). It was verified that there was no significant relative movement between the probe and the specimen when tests were running. The probe was shielded by a cylindrical Mu metal tube to reduce the magnetic interference created by the external environment. By this means, the background noise level was kept to values that were smaller than 0.2 mG. The probe was placed in such a position that the distance between the surface of the specimen and the tip of the probe was approximately 1.27 cm. It was also a position that the maximum fatigue damage zone coincided with the region of optimum probe sensitivity. More detailed descriptions of the experimental setup can be found in (Erber *et al.*, 1993; 1997; Guralnick *et al.*, 2008; Bao *et al.*, 2010) and in a series of theses (Michels, 1991; Desai, 1994; Agar, 1998; Berktan, 1998; Bao, 2004; 2007).

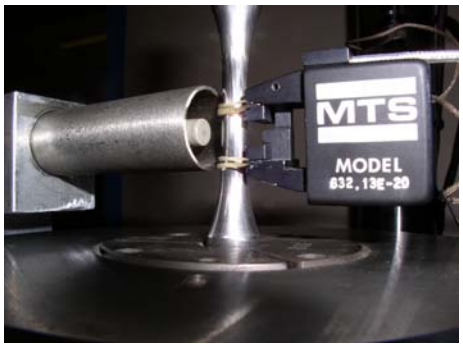

Fig. 1 Experimental setup of extensometer and fluxgate magnetometer. The magnetometer probe was shielded by a cylindrical Mu metal tube to reduce the magnetic interference. Rubber bands were used to install the extensometer

All of the experiments were run under total strain control using symmetric triangular waveforms. For fatigue tests with $N_f<7\times10^4$, a push-pull frequency of 0.5 Hz and a data sampling rate of 1000 points/cycle were used. For fatigue tests with $N_f>7\times10^4$, the push-pull frequency was increased to 1 Hz and the data sampling rate was reduced to 300 points/cycle (Bao, 2007). Test specimens with dimensions shown in Fig. 2 were machined from a single bar of cold-finished unannealed AISI 1018 steel. This material does not have a sharply defined yielding point. It has good case hardening properties and is excellent for bending and cold forming. A high-speed tracer lathe equipped with a carbide cutting tool was used to make the specimens. These were hand polished to remove any scratches that were visible under a 2X magnifier. Fig. 3 shows the magnetic fields surrounding a specimen before loadings are applied. Curve A is the magnetic measurements when the probe is positioned perpendicularly to the specimen and 1.27 cm away from the specimen surface. Curve B is the magnetic measurements when the probe is perpendicularly positioned 2.54 cm away from the surface of the specimen. The chemical compositions of this steel are shown in Table 1. The mechanical properties obtained from ten axial tension tests are shown in Table 2. The root mean square scatter of these results was approximately 2.3% without any obvious outliers. These results are consistent with those described in the American Society for Metals (II-1986).

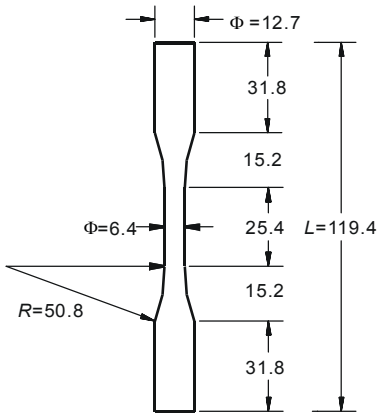

Fig. 2 Fatigue specimen dimensions (unit: mm)

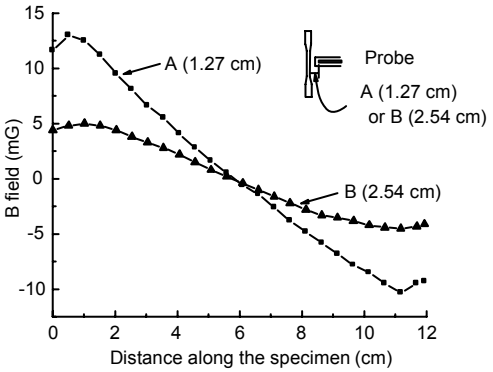

Fig. 3 Magnetic fields surrounding a specimen before test is started. Curves A and B are the magnetic measurements with the probe positioned 1.27 and 2.54 cm respectively away from the specimen surface

Table 1 Chemical compositions of AISI 1018 steel

Element	Weight (%)	Element	Weight (%)
C	0.160	Ni	0.04
Mn	0.750	Cr	0.04
P	0.012	Cu	0.06
S	0.016	Mo	0.02
Si	0.040	Fe	98.86

Table 2 Mechanical properties of AISI 1018 steel

Parameter	Value
Modulus of elasticity	210 GPa
0.2% offset yield strength	490 MPa
Proportional limit	330 MPa
Endurance (fatigue) limit	<262 MPa
Ultimate tensile strength	540 MPa

3 Results and discussion

As a representative illustration of the experimental results, fatigue test specimen 244 (Fts244) with a strain range of 0.004 and a fatigue life of 105 736 cycles is elaborated here. To preserve continuity with the experimental measurements previously undertaken at the Illinois Institute of Technology, the test specimen designations (e.g., Fts244) are identical with those cited in earlier publications (Guralnick *et al.*, 2008). Fig. 4 displays the first two strain-B field hysteresis loops illustrating the marked changes of the magnetic hysteresis traces during the initial fatigue stage. The significant changes of the magnetic hysteresis are a reflection of the material's drastic internal adjustment to the external loading. There are two sets of reversal points in each loading cycle (Fig. 4). In the initial loading, an increase followed by a decrease of the piezomagnetic field was observed and these crossover points are known as the Villari reversals (Villari, 1865). During unloading, the non-monotonic behavior of the piezomagnetic field measurement was demonstrated again and they are denoted as Tail reversals in this discussion. Detailed descriptions of the Villari effects can also be found in (Smaga *et al.*, 2008). In Fig. 4, Villari reversal 2 is dramatically shifted from Villari reversal 1 with a strain increase of 0.001 25 which is approximately 31% of the total strain range. The initial slope of the strain-magnetic field trace is approximately 8000 mG and appears to exhibit a dependence on strain rate. This needs to be investigated more thoroughly because the magnetic field probes were not uniformly oriented in all the tests. Table 3 shows the initial slope of the magnetic trace and the shift of the first two Villari reversals along the strain axis. In Fig. 4, the maximum B field of the Villari reversals is increased from 3.0 mG in cycle 1 to 3.5 mG in cycle 2. The maximum B field of the Tail reversals is increased significantly from

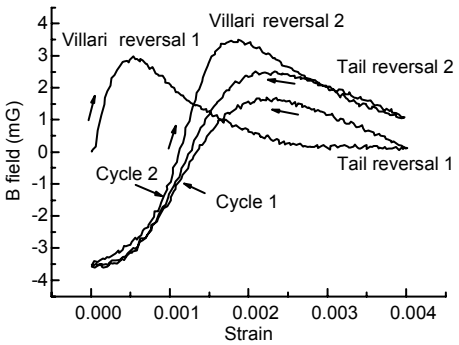

Fig. 4 First two strain-B field hysteresis loops of test Fts244 illustrating the dramatic changes of the magnetic hysteresis traces that occur during the initial accommodation stage

Table 3 Initial slope of the magnetic trace and shift of the first two Villari reversals

Test	Fatigue life	Strain range $\Delta\varepsilon$	Strain shift $\Delta\varepsilon_s$	$\Delta\varepsilon_s/\Delta\varepsilon$ (%)	Initial slope (mG)
Fts228	3362	0.0105	0.00238	22.7	3200
Fts229	7505	0.0080	0.00209	26.1	7200
Fts230	13300	0.0070	0.00196	28.0	4500
Fts231	4400	0.0090	0.00220	24.4	4800
Fts232	21500	0.0055	0.00135	24.5	3300
Fts233	3561	0.0105	0.00295	28.1	4500
Fts234	3550	0.0105	0.00260	24.8	4500
Fts243	50770	0.0052	0.00185	35.6	7900
Fts244	105736	0.0040	0.00125	31.0	8000
Fts247	76033	0.0043	0.00144	33.5	8000

1.7 mG in cycle 1 to 2.5 mG in cycle 2 although the Tail reversals remain relatively stable along the strain axis. Fig. 5 displays the piezomagnetic hysteresis traces from cycle 5000 to cycle 5005. M' is the field maximum of the Villari reversals shown in Fig. 4, I' is the intersection of the piezomagnetic traces corresponding to the increasing and decreasing parts of the strain cycle. Comparing Fig. 4 and Fig. 5, one can see that the magnetic hysteresis loops have been moved up along the B field axis. The 'head' of the magnetic hysteresis loop is increased from −3.5 to −2.6 mG; the 'tail' of the magnetic hysteresis loop is increased from 0.1 to 1.8 mG. The field maximum of the Villari reversals M' increases from 3.0 to 4.4 mG. Fig. 6 displays the strain-B field hysteresis traces from cycle 13000 to cycle 13005 which is in the vicinity of N_2. An overlay of Fig. 5 and Fig. 6 shows that the shapes of the magnetic hysteresis loops tend to become wider and the position of the hysteresis loops has been moved up along the B field axis. In Fig. 6, the 'head' of hysteresis loops has a value of −2.3 mG, and the 'tail' has a value of 1.9 mG. Figs. 4–6 demonstrate the development of the piezomagnetic field during the initial accommodation stage of fatigue. Figs. 7 and 8 show the strain-magnetic field traces from cycle 53000 to cycle 53005 and from cycle 97000 to cycle 97005 in the accretion of damage stage. An overlay of these two figures shows that the magnetic hysteresis loops remain relatively stable in terms of shape and position of the traces. The 'head' of hysteresis loop increases slightly from −1.8 mG in cycle 53000 to −1.5 mG in cycle 97000. The 'tail' of the loop moves slightly down from 1.7 mG in cycle 53000 to 1.6 mG in cycle 97000. The field maximum of the Villari reversals M' remains at 4.5 mG in cycle 53000 and in cycle 97000. In contrast to the drastic changes of the piezomagnetic traces in the initial fatigue stage, the relatively stable response of the magnetic hysteresis in the accretion of damage stage demonstrates a very slow but steady accumulation of damage in the material's mesostructure. In the terminal failure stage, the material starts to degrade rapidly and this is reflected in conspicuous changes in the strain-B field traces. Fig. 9 shows the magnetic response from cycle 105730 to cycle 105736. Comparing Fig. 8 and Fig. 9, it can be observed that the 'head' of hysteresis loop in cycle 105730 has a totally different shape compared to that in cycle 97000. The 'tail' of the hysteresis loop moves further down from 1.6 mG in cycle 97000 to 1.0 mG in cycle 105730. The field maximum of the Villari reversals M' decreases from 4.5 mG in cycle 97000 to 3.6 mG in cycle 105730. The intersection point I' shifts along the strain axis from 0.0026 to 0.0034. In Fig. 9, the conspicuous opening of the intervals between adjacent traces reflects the rapid rate of deterioration of material strength during terminal

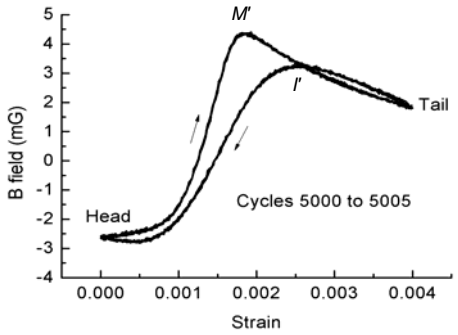

Fig. 5 ε-B hysteresis loops for cycles 5000–5005 of test Fts244

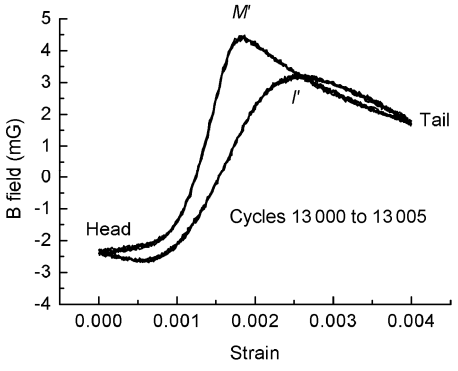

Fig. 6 ε-B hysteresis loops for cycles 13000–13005 of test Fts244

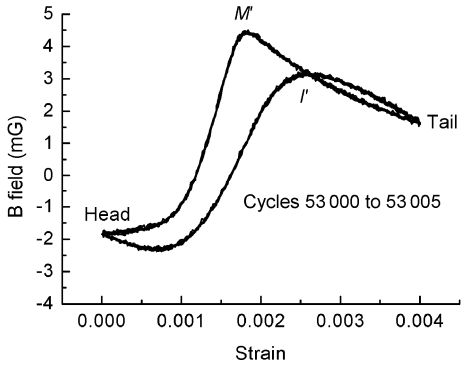

Fig. 7 ε-B hysteresis loops for cycles 53 000–53 005 of test Fts244

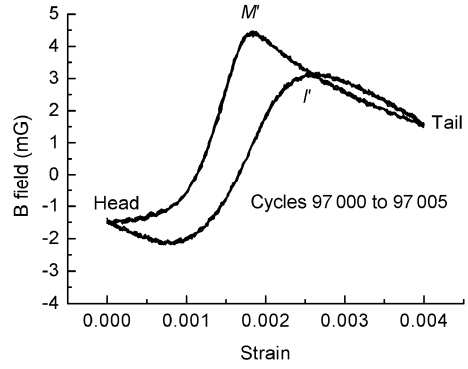

Fig. 8 ε-B hysteresis loops for cycles 97 000–97 005 of test Fts244

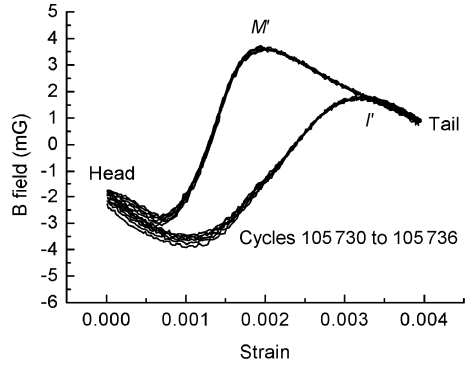

Fig. 9 ε-B hysteresis loops for cycles 105 730–105 736 of test Fts244 illustrating the opening of the intervals between adjacent curves during terminal failure

failure. The drastic changes of the piezomagnetic traces in the late stage of fatigue are an early warning of the failure of the material.

The above-mentioned has shown that the piezomagnetic traces evolve constantly in terms of shape and position over the entire course of the fatigue degradation process. A computer program was developed to quantitatively identify the movement of the strain-B field hysteresis traces. Results show that the evolution of the 'tail' of the piezomagnetic hysteresis loop follows a predictable course. Fig. 10 shows the B fields of the 'tail' of the magnetic hysteresis loops plotted against the number of loading cycles for test Fts230. It can be clearly seen from this figure that the B field curve first increases rapidly, then relaxes to a more gradual rate of change, and finally in the terminal stage, a rapid variation occurs again. This trend is consistent with the evolution of the mechanical hysteresis loop areas which has been extensively investigated (Michels, 1991; Desai, 1994; Agar, 1998; Berktan, 1998; Bao, 2004; 2007; Giancane *et al.*, 2010). Utilizing the algorithms described by Guralnick *et al.* (2008), it is possible to identify two transition points, N_{2PM} and N_{3PM}, analogous to the N_{2A} and N_{3A} divisions found previously in stress-strain hysteresis. The results in Table 4, which are obtained by analysis of the piezomagnetic hysteresis traces, show that the ratios N_{2PM}/N_f and N_{3PM}/N_f tend to be stable although the specific N_{2PM} and N_{3PM} values vary from test to test. In Table 4, the average N_{2PM}/N_f ratio is 11.5% and the average N_{3PM}/N_f ratio is 92.2%. The data in Table 5, which are obtained by studies of the mechanical hysteresis loop areas, show that the average ratio of N_{2A}/N_f is 11.4% and the average ratio of N_{3A}/N_f is 92.0%. Similar treatments of N_2/N_f and N_3/N_f based on stress-strain measurements can also be found in (Walther and Eifler, 2007). Table 4 and Table 5 show that the ratios of N_2/N_f and N_3/N_f obtained from magnetic hysteresis are quite consistent with those obtained from mechanical hysteresis. Detailed comparisons of N_2 and N_3 values obtained from analysis of the stress-strain hysteresis and the strain-B field hysteresis can be observed in Fig. 11 and Fig. 12. Fig. 11 is a graph of values of N_{2A} obtained from the evolution of mechanical hysteresis loop areas versus N_{2PM} obtained from the evolution of the 'tail' of the magnetic hysteresis traces. The solid line represents that N_{2A} from mechanical hysteresis perfectly matches N_{2PM} from magnetic hysteresis. It can be seen from this figure that N_{2A} values from mechanical hysteresis correspond well with those from magnetic hysteresis. The plot of N_{3A} from mechanical hysteresis versus N_{3PM} from magnetic hysteresis is presented in Fig. 12. One can find that N_{3A} values from mechanical hysteresis correspond very closely with those from magnetic

hysteresis. It is good to see an approximate consistency between datasets derived from two rather different physical effects.

Table 4 Fatigue test results (evolution of the 'tail' of the strain-B field hysteresis loop)

Test	Strain range	N_f	N_{2PM}	N_{2PM}/N_f (%)	N_{3PM}	N_{3PM}/N_f (%)
Fts228	0.0105	3362	384	11.4	3152	93.8
Fts233	0.0105	3561	412	11.6	3209	90.1
Fts234	0.0105	3550	385	10.8	3126	88.1
Fts231	0.0090	4400	417	9.50	3956	89.9
Fts229	0.0080	7505	946	12.6	7017	93.5
Fts230	0.0070	13300	1503	11.3	12055	90.6
Fts232	0.0055	21500	2842	13.2	20349	94.6
Fts243	0.0052	50770	5879	11.6	47856	94.3
Fts247	0.0043	76033	8329	11.0	70916	93.3
Fts244	0.0040	105736	13153	12.4	97554	92.3
Fts252	0.0035	189629	21768	11.5	177382	93.5
Average				11.5		92.2

Table 5 Fatigue test results (evolution of the stress-strain hysteresis loop area)

Test	Strain range	N_f	N_{2A}	N_{2A}/N_f (%)	N_{3A}	N_{3A}/N_f (%)
Fts228	0.0105	3362	447	13.3	2983	88.7
Fts233	0.0105	3561	387	10.9	3190	89.6
Fts234	0.0105	3550	387	10.9	3255	91.7
Fts231	0.0090	4400	483	11.0	3875	88.1
Fts229	0.0080	7505	762	10.2	7049	93.9
Fts230	0.0070	13300	989	7.40	11526	86.7
Fts232	0.0055	21500	2189	10.2	19621	91.3
Fts243	0.0052	50770	5153	10.2	48308	95.2
Fts247	0.0043	76033	11570	15.2	74362	97.8
Fts244	0.0040	105736	14334	13.6	99181	93.8
Fts252	0.0035	189629	23014	12.1	180495	95.2
Average				11.4		92.0

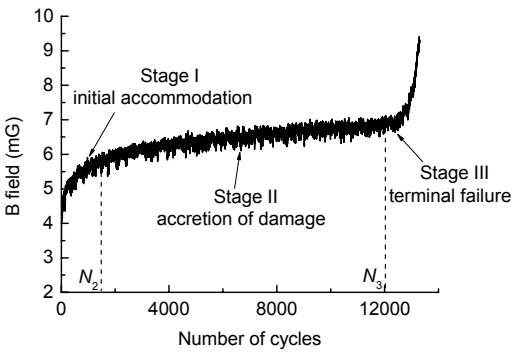

Fig. 10 B field of the 'tail' of piezomagnetic hysteresis loops for test Fts230. The evolution of the 'tail' of piezomagnetic hysteresis has three principal stages

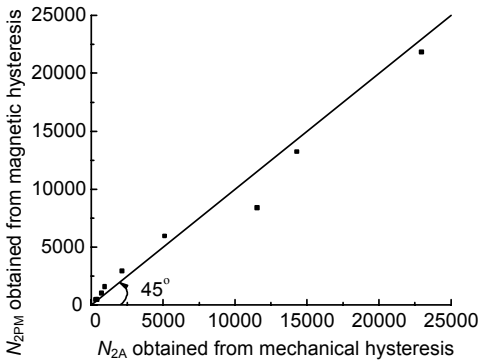

Fig. 11 N_{2A} from mechanical hysteresis vs. N_{2PM} from magnetic hysteresis

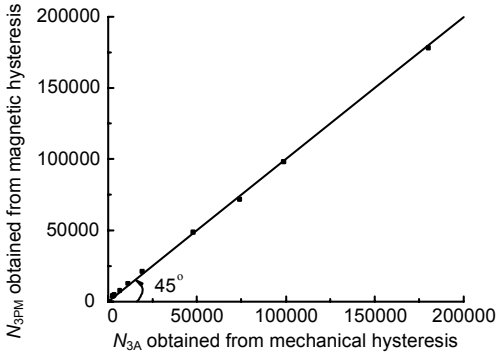

Fig. 12 N_{3A} from mechanical hysteresis vs. N_{3PM} from magnetic hysteresis

4 Conclusions

The basis for the present analysis consists of 11 experiments conducted to study the correlations between the piezomagnetic fields surrounding AISI 1018 steel specimens and fatigue. Extensive studies of the magnetic responses of these 11 tests show that there are systematic changes in terms of the shape and position of the magnetic traces in each experiment. Statistical analysis show that the evolution of the 'tail' of the piezomagnetic traces follows the three principal stages of fatigue: initial accommodation, accretion of damage, and terminal failure. The piezomagnetic traces show conspicuous changes in the initial stage, then revert to a relatively stable phase, and finally, drastic variations appear again. Curve fitting of the data was then carried out to determine the transitions of the three stages, N_{2PM} and N_{3PM}. It was found that although N_{2PM} and N_{3PM} values vary widely, the ratio values of N_{2PM}/N_f and N_{3PM}/N_f are relatively stable, N_{2PM}/N_f=11.5% and N_{3PM}/N_f=92.2%. All of

these results are consistent with those obtained from analysis of the mechanical hysteresis traces, i.e., N_{2A}/N_f=11.4% and N_{3A}/N_f=92.0%. The relationships between N_2 and N_f as well as N_3 and N_f appear to provide very simple yet reasonably reliable fatigue failure prediction methods, i.e., $N_f \approx 8.7N_2$ and $N_f \approx 1.08N_3$.

Further research is needed to investigate if piezomagnetic effects can improve the accuracy of mechanical failure predictions. Research may also be carried out to study if the piezomagnetic field follows a predictable course for a fixed strain range. Finally, the results in this research show that the initial slope of the strain-magnetic field trace seems to be dependent on strain rate. This needs to be investigated more thoroughly.

References

Agar, B.B., 1998. Hysteresis and Low Cycle Fatigue in Selected Aluminum Alloys. MS Thesis, Illinois Institute of Technology, Chicago, IL.

American Society for Metals (II-1986), 1986. Metals Handbook. Carnes Publication Services Inc.

Bannantine, J.A., Comer, J.J., Handrock, J.L., 1990. Fundamentals of Metal Fatigue Analysis. Prentice Hall, New Jersey.

Bao, S., 2004. Two-parameter Characterization of Low Cycle, Hysteretic Fatigue Data. MS Thesis, Illinois Institute of Technology, Chicago, IL.

Bao, S., 2007. Fatigue, Mechanical and Magnetic Hysteresis. PhD Thesis, Illinois Institute of Technology, Chicago, IL.

Bao, S., Jin, W.L., Guralnick, S.A., Erber, T., 2010. Two-parameter Characterization of Low Cycle, Hysteretic Fatigue Data. *Journal of Zhejiang University-SCIENCE A (Applied Physics and Engineering)*, **11**(6):449-454. [doi:10.1631/jzus.A0900763]

Becker, R., Doring, W., 1939. Ferromagnetismus. Springer, Berlin.

Berktan, T., 1998. Piezomagnetism and Fatigue. MS Thesis, Illinois Institute of Technology, Chicago, IL.

Bily, M., 1993. Cyclic Deformation and Fatigue of Metals. Elsevier, Amsterdam.

Bozorth, R.M., 1951. Ferromagnetism. van Nostrand Co., Princeton, NJ.

Cullity, B.D., 1972. Introduction to Magnetic Materials. Addison-Wesley Publishing Co., MA.

Desai, R.D., 1994. Origin and Inception of Fatigue Damage in Steel. MS Thesis, Illinois Institute of Technology, Chicago, IL.

Erber, T., 2001. Hooke's law and fatigue limits in micromechanics. *European Journal of Physics*, **22**(5):491-499. [doi:10.1088/0143-0807/22/5/305]

Erber, T., Guralnick, S.A., Michels, S.C., 1993. Hysteresis and fatigue. *Annals of Physics*, **224**(2):157-192. [doi:10.1006/aphy.1993.1043]

Erber, T., Guralnick, S.A., Desai, R.D., Kwok, W., 1997. Piezomagnetism and fatigue. *Journal of Physics D: Applied Physics*, **30**(20):2818-2836. [doi:10.1088/0022-3727/30/20/008]

Giancane, S., Panella, F.W., Dattoma, V., 2010. Characterization of fatigue damage in long fiber epoxy composite laminates. *International Journal of Fatigue*, **32**(1):46-53. [doi:10.1016/j.ijfatigue.2009.02.024]

Guralnick, S.A., Bao, S., Erber, T., 2008. Piezomagnetism and fatigue: II. *Journal of Physics D: Applied Physics*, **41**(11):115006. [doi:10.1088/0022-3727/41/11/115006]

Kachanov, L.M., 1986. Introduction to Continuum Damage Mechanics. Martinus Nijhoff, Dordrecht, the Netherlands.

Lemaitre, J., Chaboche, J.L., 1990. Mechanics of Solid Materials. Cambridge University Press, Cambridge, UK.

Michels, S., 1991. Hysteresis and Fatigue. MS Thesis, Illinois Institute of Technology, Chicago, IL.

Smaga, M., Walther, F., Eifler, D., 2008. Deformation-induced martensitic transformation in metastable austenitic steels. *Materials Science and Engineering A*, **483-484**:394-397. [doi:10.1016/j.msea.2006.09.140]

Villari, E., 1865. Change of magnetization by tension and by electric current. *Annual Physics Chemistry*, **126**:87-122.

Walther, F., Eifler, D., 2007. Cyclic deformation behavior of steels and light-metal alloys. *Materials Science and Engineering A*, **468-470**:259-266. [doi:10.1016/j.msea.2006.06.146]